



Single-stage direct Langevin dynamic simulations of transitions over arbitrarily high energy barriers: Concept of energy-dependent temperature

Dmitry Berkov , Elena K. Semenova, and Natalia L. Gorn
General Numerics Research Lab, Leutragraben 1, D-07743 Jena, Germany

 (Received 9 August 2021; revised 19 October 2021; accepted 8 November 2021; published 7 December 2021)

In this paper we present an algorithm which allows *single-stage* direct Langevin dynamics simulations of the escape rate over *arbitrarily high* energy barriers employing the concept of the energy-dependent temperature (EDT). In our algorithm, simulation time required for the computation of the escape rate *does not increase* with the energy barrier. This is achieved by using in simulations an effective temperature which depends on the system energy: around the energy minima this temperature is high, whereas it tends towards room temperature when the energy approaches the saddle point value. Switching times computed via our EDT algorithm show an excellent agreement with results obtained with the established forward flux sampling (FFS) method. As the simulation time required by our method does not increase with the energy barrier, we achieve a very large speedup when compared even to our highly optimized FFS version with interfaces placed equidistantly in the energy space. In addition, our method does not suffer from stability problems occurring in multistage algorithms (like FFS and “energy bounce” methods) due to the multiplication of a large number of transition probabilities between the interfaces.

DOI: [10.1103/PhysRevB.104.224408](https://doi.org/10.1103/PhysRevB.104.224408)

I. INTRODUCTION

Evaluation of escape rates Γ (or, equivalently, switching times $\tau_{\text{sw}} = 1/\Gamma$) over high energy barriers is a highly important and in most cases a very difficult task arising in any scientific area where systems with more than one stable state are studied—in physics, chemistry, molecular biology, material science, etc. [1]. The large variety of corresponding applications—including catalytic reactions (in particular protein folding), diffusion in systems with high energy barriers, phase transitions, and information stability in any type of storage media—is considered in many recent books and reviews, see, e.g., [2–6].

System dynamics near the saddle point may be highly nontrivial, so that evaluating the transition rate is much more difficult than the computation of the height of the corresponding energy barriers ΔE separating metastable energy minima. For solution of the latter problem, several meanwhile standard methods have been implemented in recent decades. The most widely used algorithm for this purpose is undoubtedly the “nudged elastic band” (NEB) method of Jonsson *et al.* [7], which employs the idea that the energy gradient component perpendicular to the optimal path should be zero along the whole path. The main advantage of NEB is that neighboring system states along the transition path are connected via artificial “springs” to prevent a too large distance between these states during the path-finding procedure. Examples of the latest generalizations and improvements of this powerful method and its applications to very different chemical systems—from chemical reactions over dislocation dynamics to magnetic transitions—can be found, e.g., in [8–12].

Some less known methods for computing ΔE are the closely related “string method” which also searches for the

“minimal energy path,” but in a slightly different way [13,14] and the minimization of the Onsager-Machlup functional [15], first implemented by us for an interacting system of magnetic single-domain particles in [16].

In order to compute the average lifetime of a system with several metastable states— which is the real quantity of interest for most applications—one needs more than the value of the energy barrier ΔE . Even in the simplest analytical approximation for Γ given by the Arrhenius law $\Gamma = \nu_{\text{att}} \exp(\Delta E/k_{\text{B}}T)$, the “attempt frequency” ν_{att} , usually interpreted as the oscillation frequency near the metastable state, is present. Omitting the discussion about the difficult task of computing this frequency for systems with internal degrees of freedom (see, e.g., [1,17,18], etc.), we recall that the Arrhenius law is fundamentally not a satisfactory approach [19,20]: this law does not contain the system damping, in which presence in the escape rate is required by the fluctuation-dissipation theorem, as switching can occur only due to the interaction with the thermal bath.

The best possible analytical solution for the escape rate in a system with arbitrary damping (known as the Kramers problem) was derived in the famous paper of Mel’nikov and Meshkov [21]; this solution includes the intermediate-to-high damping (IHD) regime studied by Brown [22] and the very low damping (VLD) considered by Klik and Günther [23]. The formalism developed in [21] was successfully applied to escape rates out of a single well and transition rates between two energy minima for a single-domain magnetic particle in [24,25]; for the corresponding detailed review see [20].

However, as any analytical approach, this solution has serious shortcomings. Many-particle systems with strong interparticle interaction usually cannot be studied analytically, even when only one interaction type is dominating (like

Coulomb interaction in systems of charged particles). Within the context of this study, an analytical solution is not available for magnetic particles with a size larger than the characteristic micromagnetic length [26], so that magnetization configuration of these particles is spatially nonhomogeneous. In this case, some discretization is required, leading to a system of strongly interacting mesh-based entities. An additional problem arises due to the presence of several micromagnetic energy contributions (in particular, the competition between the strong short-range exchange and long-range magnetodipolar interactions), which makes even the straightforward solution of the Landau-Lifshitz-Gilbert equation of motion in such systems a highly demanding task.

Hence general numerical methods for the evaluation of the actual escape rate for many-particle systems in general and for magnetic systems in particular are strongly desired. Among these methods, the Langevin dynamics (LD) is conceptually the simplest one, because it directly mimics the time evolution of the system under the influence of thermal fluctuations. Unfortunately, exactly for this reason LD is suitable for small barriers only ($\Delta E/k_B T \leq 10$), because switching times (and correspondingly the computation time) grow exponentially with ΔE .

Thus, working methods for evaluating numerically the escape rate over high barriers are usually based on a kind of gradual “climbing” towards the saddle point uphill the energy surface.

The most successful general method of this class is the so called forward flux sampling (FFS) [27–30]. In FFS, the phase space between the two energy minima of interest is first divided into a (large) number of interfaces. Then the probability $w(\lambda_i \rightarrow \lambda_{i+1}) \equiv w_{i \rightarrow i+1}$ to reach the next interface starting from the previous one is computed. In order to ensure that this probability is computed reasonably fast and accurately by standard LD simulations, subsequent interfaces are placed relatively close to each other. Finally, multiplying the product of all these transition probabilities (i.e., for all interface pairs between the two minima) by the flux out of the starting minimum through the first interface, one obtains the transition rate.

The interfaces are usually defined in the system coordinate space, using the sequence of values of the “reaction coordinate” or the “order parameter,” which defines whether the transition has occurred or not. In micromagnetics, this method was applied for magnetization switching in columnar recording structures (order parameter being the average magnetization projection) [31–33] and in skyrmions (order parameter was the skyrmion size) [34].

Computational time for a single FFS run is roughly proportional to the energy barrier height, because for larger barriers more interfaces are needed in order to maintain the transition probabilities between the neighboring interfaces reasonably high. However, an additional (and often really substantial) time effort is required for the optimal positioning of interfaces. This optimal positioning should ensure that transition probabilities $w_{i \rightarrow i+1}$ are at least approximately the same for all interface pairs, because in this case the most accurate estimation of the transition rate is achieved [29,30]. Corresponding optimal placement uses an iterative procedure which naturally requires several evaluations of the whole set of these

probabilities, i.e., several complete FFS runs. We could demonstrate [35] that this large additional effort can be avoided if the interfaces are placed directly in the energy space, so that all probabilities $w_{i \rightarrow i+1}$ (which are $\sim \exp[-(E_{i+1} - E_i)/k_B T]$) are approximately equal.

Another inherent problem of FFS and related multistage climbing methods (e.g., the “energy bounce” (EnB) algorithm [36]) is the tight requirement to the accuracy of the numerically computed transition probabilities w_i , usually evaluated by LD simulations. This accuracy should be really high because the final result includes the product of these probabilities so that any bias of w_i from a system with N interfaces will be elevated to the N th degree. Systematic errors are especially dangerous—it is easy to estimate that for a system with 50 interfaces, such an error of only 2% in each w_i would lead to the error of nearly 300% in the final result. Even the stochastic mean-square error of only 5% on each interface—a very good value for this kind of simulation—would lead to a relative error of $\approx 35\%$ in the computed switching rate.

Thus, a new class of numerical methods which could perform the evaluation of the switching rate over the energy barriers of arbitrary heights using only *single-stage* Langevin dynamics simulations (in contrast to a gradual “climbing” over a long series of interfaces as in FFS and EnB algorithms) is highly desirable. In this study we present such an algorithm, introducing the concept of the energy-dependent effective temperature. Our method allows stable and accurate single-stage simulations of transitions over any barrier with the simulation time which *does not increase* with the barrier height.

This paper is organized as follows. In Sec. II A we describe the main idea of our algorithm. It is based on LD simulations of the system where the effective temperature depending on the system energy (EDT) is introduced: this temperature is high near the energy minima and tends to room temperature in the vicinity of the saddle point(s). Then, in Sec. II B we derive the relation between the switching time τ_{sw}^{EDT} obtained for the EDT system and the “real” switching time τ_{sw}^{CT} for the system at constant temperature (CT). In Sec. III the Markov chain used for the evaluation of the ratio of probability products for EDT and CT cases is constructed. Section IV is devoted to the validation of our method via the EDT version of the FFS algorithm. Finally, Sec. V contains the direct comparison of real switching times obtained by EDT and standard ($T = \text{const.}$) FFS algorithms. Here we show a very good agreement between both methods in the energy barriers interval $10 \leq \Delta E/k_B T \leq 60$, where switching times span about 20 orders of magnitude. Furthermore, we demonstrate a large speedup of the EDT algorithm as compared even to the optimized (as explained in [35]) FFS method.

The short version of this research is submitted elsewhere [37].

II. ENERGY-DEPENDENT TEMPERATURE: METHODOLOGY

A. Main idea

Direct LD simulations of transitions over high energy barriers are not feasible due to the major drawback of this

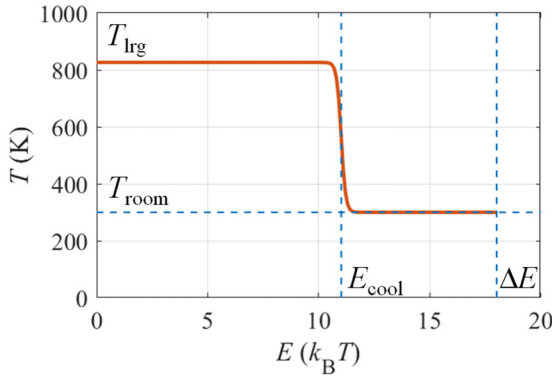


FIG. 1. Effective temperature as a function of energy; in this example $\Delta E/k_B T = 18$, $a_{1rg} = 4$, $b_{cool} = 7$.

method: the system spends the overwhelming majority of time in the vicinity of its energy minima, because the probability to approach the landscape region near the saddle point is exponentially small [$p \sim \exp(-\Delta E/k_B T)$].

To overcome this obstacle, we suggest to introduce the effective energy-dependent temperature $T(E)$, which depends on the system energy in the following way. For energies close to the saddle point, $T(E)$ is equal to the temperature at which we would like to compute the escape rate—we denote it as room temperature T_{room} , so that $T(E) \rightarrow T_{room}$ for $\Delta E - E \sim k_B T$. For energies considerably lower than the energy barrier, $T(E)$ is much higher than T_{room} : $T(E) = T_{1rg} \gg T_{room}$ for $\Delta E - E \gg k_B T$.

For this purpose, we use the functional dependence

$$T(E) = a_1 + a_2 \tanh\left(\frac{\Delta E - b_{cool} k_B T}{\Delta_T}\right) \quad (1)$$

(see Fig. 1). The finite width Δ_T of this T distribution should merely ensure a smooth transition between the “hot” and “cold” regions (abrupt temperature change would cause numerical instabilities of LD trajectories); we have checked that values $\Delta_T = (0.1-1.0)k_B T$ lead to the same final results. Parameters a_1 and a_2 should be chosen to satisfy the two conditions

$$\begin{aligned} T(E : E - E_{cool} \gg k_B T) &\rightarrow T_{room}, \\ T(E : E_{cool} - E \gg k_B T) &\rightarrow T_{1rg} \end{aligned} \quad (2)$$

(cold region near the barrier and hot region far below the barrier), so that $a_1 = (T_{room} + T_{1rg})/2$ and $a_2 = (T_{room} - T_{1rg})/2$.

The performance of the method, i.e., its speed, and hence the statistical accuracy of the result, is controlled by parameters T_{1rg} and b_{cool} . First of all, the temperature T_{1rg} and the “cooling” energy $E_{cool} = \Delta E - b_{cool} k_B T_{1rg}$ determine the probability $p_{cool} \approx \exp(-E_{cool}/k_B T_{1rg})$ to occupy the states near E_{cool} (the latter relation does not take into account the energy dependence of the density of states, but this dependence is much weaker than the exponential factor). This probability should be large enough to frequently provide “launching points” for the system in order to overcome the effective energy barrier $\Delta E_{eff} = \Delta E = E_{cool}$ starting from these states. We have found that the values p_{cool} in the region $p_{cool} = 0.002-0.02$ are the optimal choice, resulting in $E_{cool}/k_B T_{1rg} =$

$a_{1rg} \approx 4-6$. Increase of a_{1rg} (i.e., decrease of T_{1rg}) above this range naturally led to fewer observed transitions and poorer statistics. Smaller values of a_{1rg} led to values of T_{1rg} which are so high that the system behavior near the saddle point was still affected. We shall explain this issue in more details in Sec. IV. For results presented below we have used $a_{1rg} = 4$.

The last parameter to be determined (b_{cool}) controls the height of the effective energy barrier $\Delta E_{eff} = b_{cool} k_B T_{room}$ which the system has to overcome starting from the energy E_{cool} . Hence the number of transitions observed during the EDT simulations exponentially depends on this parameter. For this reason the upper limit of b_{cool} is set simply by the largest barrier which can be overcome within standard LD simulations: $\Delta E_{eff} \leq 10 k_B T$, so that $b_{cool} \leq 10$. On the other hand, too small values of b_{cool} lead to very frequent crossings of the energy barrier, so that the very idea of studying rare events is lost (in particular, the system cannot reach a partial equilibrium within the given energy well). From the methodical point of view, it becomes hardly possible to distinguish between “true” and “false” transitions between the basins (see [35] for the detailed discussion). This argument sets the low limit as $b_{cool} \geq 5$. In our simulations we have used mostly $b_{cool} = 7$ and have checked that varying it in the above mentioned limits does not change the final results within the statistical accuracy.

Taking into account that we have used only general “thermodynamical” arguments to choose these parameters, we believe that our choice should be valid (at least as a good first approximation) also for other physical systems.

An example of the dependence $T(E)$ with parameters given above is shown in Fig. 1 for a system with the energy barrier $\Delta E = 18 k_B T$.

It is clear that for the system with the EDT profile (1) we should observe numerous transitions over the barrier ΔE by employing direct LD simulations, no matter how large this barrier is: effective temperature for energies $E < \Delta E - b_{cool} k_B T$ is high enough to ensure a significant occupation of these states, so that the energy barrier to be overcome is only $\Delta E^{EDT} \simeq b_{cool} k_B T$. The corresponding switching time for an EDT system thus can be computed in a standard way using LD simulations, namely dividing the physical simulation time by the number of true switchings: $\tau_{sw}^{EDT} = t_{sim}/M_{sw}$ [35].

The key problem is how to establish the relation between this EDT-computed switching time τ_{sw}^{EDT} and the switching time for the same system at a constant temperature τ_{sw}^{CT} —the quantity of a real physical interest.

B. Relation between the EDT-computed time and the real switching time

To establish this relation, we start from the same expression for the transition rate Γ which is used in forward-flux sampling (FFS): we introduce virtual interfaces $\{\lambda_i, i = 1, \dots, N\}$ between the basins **A** and **B** (whereby $\lambda_1 \equiv \lambda_A$, $\lambda_N \equiv \lambda_B$), so that

$$\Gamma_{A \rightarrow B} = \Phi_{\lambda_1 \rightarrow \lambda_2} \prod_{i=2}^{N-1} w(\lambda_i \rightarrow \lambda_{i+1}) \equiv \Phi_A \prod_{i=2}^{N-1} w_{i \rightarrow i+1}. \quad (3)$$

This equation represents a very general statement (not restricted to FFS) that the transition rate $\Gamma_{\mathbf{A} \rightarrow \mathbf{B}}$ can be computed as the product of the flux $\Phi_{\mathbf{A}}$ out of the basin \mathbf{A} through the interface λ_2 (i.e., the number of particles per unit time starting in \mathbf{A} and crossing the first interface outside \mathbf{A}), and the subsequent conditional probabilities $w_{i \rightarrow i+1}$ that a particle starting from the interface i reaches the interface $i+1$. Note that we slightly changed the numbering of the interface compared to our previous paper [35] to make it consistent with the numbering of Markov chain states used in the next sections.

Using Eq. (3) and the relation $\tau_{\text{sw}} = 1/\Gamma$, the ratio of interest can be written as

$$\frac{\tau_{\text{sw}}^{\text{CT}}}{\tau_{\text{sw}}^{\text{EDT}}} = \frac{\Gamma_{\mathbf{A} \rightarrow \mathbf{B}}^{\text{EDT}}}{\Gamma_{\mathbf{A} \rightarrow \mathbf{B}}^{\text{CT}}} = \frac{\Phi_{\mathbf{A}}^{\text{EDT}}(T = T_{\text{lg}}) \prod_{i=2}^{N-1} w_{i \rightarrow i+1}^{\text{EDT}}}{\Phi_{\mathbf{A}}^{\text{CT}}(T = T_{\text{room}}) \prod_{i=2}^{N-1} w_{i \rightarrow i+1}^{\text{CT}}}, \quad (4)$$

where the initial fluxes should be computed at corresponding temperatures, as explicitly indicated in (4). Hence, the actual switching time can be evaluated as

$$\tau_{\text{sw}}^{\text{CT}} = \tau_{\text{sw}}^{\text{EDT}} \frac{\Phi_{\mathbf{A}}^{\text{EDT}}}{\Phi_{\mathbf{A}}^{\text{CT}}}, \quad (5)$$

where r denotes the ratio of two probability products

$$r = \frac{\prod_{i=2}^{N-1} w_{i \rightarrow i+1}^{\text{EDT}}}{\prod_{i=2}^{N-1} w_{i \rightarrow i+1}^{\text{CT}}}. \quad (6)$$

As explained above, $\tau_{\text{sw}}^{\text{EDT}}$ in expression (5) can be extracted from direct LD simulations. The fluxes $\Phi_{\mathbf{A}}^{\text{EDT}}$ and $\Phi_{\mathbf{A}}^{\text{CT}}$ are also easily available from such simulations, because the interface λ_2 is usually chosen to be close ($\sim k_B T$) to the basin \mathbf{A} . Thus, our task reduces to the evaluation of the ratio r defined by (6).

We emphasize that this ratio should be evaluated either by an analytical method or a numerical one with a very low computational effort, because otherwise the EDT algorithm will not have any advantage compared to the standard FFS. In the next section we construct a Markov chain which enables the evaluation of (6) using only N diagonalizations of matrices with sizes $\leq N$.

III. MARKOV CHAIN FORMALISM

A. Evaluation of the equilibrium probabilities $w_{i \rightarrow i+1}$ using Markov chains

In this subsection we demonstrate how to compute the required ratio (6) of probability products using the Markov chain (MCH) formalism (see, e.g., [38]). For this purpose we introduce the Markov chain with the set of states $\{i = 1, \dots, N\}$, which corresponds to our set of interfaces $\{\lambda_A = \lambda_1, \dots, \lambda_i, \dots, \lambda_N = \lambda_B\}$. We denote the *one-step* “forward” and “backward” transition probabilities between these chain states as $p_{i \rightarrow i+1}$ and $q_{i \rightarrow i-1}$. Corresponding MCH for the whole set of interfaces is shown in Fig. 2.

Properly normalized probabilities $\{p\}$ and $\{q\}$ (so that $p_{i \rightarrow i+1} + q_{i \rightarrow i-1} = 1$) form the one-step transition matrix $\hat{\mathbf{P}}$ of our MCH: $P_{i,i+1} = p_{i \rightarrow i+1}$ and $P_{i,i-1} = q_{i \rightarrow i-1}$; this matrix governs the change of the state occupations in our MCH after one step.

To compute the total transition probabilities $w_{i \rightarrow i+1}$ appearing in the basic expressions (3)–(6), we first recall how

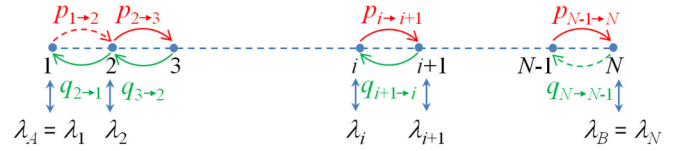


FIG. 2. Markov chain consisting of N states $\{1, \dots, N\}$ corresponding to interfaces $\{\lambda_A, \dots, \lambda_B\}$ as shown by black arrows.

these probabilities are defined: a system trajectory is started from the interface λ_i and simulated (using the standard Langevin dynamics) until it either arrives at the next interface λ_{i+1} or returns to the basin \mathbf{A} . Then the next trajectory is launched from λ_i , etc. Probability $w_{i \rightarrow i+1}$ is computed as the fraction of all launched trajectories which arrive at λ_{i+1} .

According to this procedure, the random process for which we construct our MCH for the evaluation of $w_{i \rightarrow i+1}$, terminates when the system reaches either state 1 or state $(i+1)$. Hence, for computing $w_{i \rightarrow i+1}$ we have the MCH of the length $(i+1)$ with absorbing borders, meaning that corresponding elements of the matrix $\hat{\mathbf{P}}^{(i+1)}$ of this chain are $P_{11}^{(i+1)} = P_{i+1,i+1}^{(i+1)} = 1$, $P_{12}^{(i+1)} = p_{1 \rightarrow 2} = 0$, and $P_{i+1,i}^{(i+1)} = q_{i+1 \rightarrow i} = 0$. The whole matrix $\hat{\mathbf{P}}^{(i+1)}$ is then tridiagonal and has the form

$$\hat{\mathbf{P}}^{(i+1)} = \begin{bmatrix} 1 & 0 & \dots & 0 \\ q_{21} & 0 & p_{23} & \\ 0 & q_{23} & 0 & p_{34} \\ \vdots & & \ddots & \\ & & 0 & p_{i-1,i} \\ & & q_{i,i-1} & 0 & p_{i,i+1} \\ 0 & & \dots & 0 & 1 \end{bmatrix}. \quad (7)$$

This matrix belongs to the class of stochastic matrices, for which the sum of elements of each row is one.

Next, we recall that $w_{i \rightarrow i+1}$ is computed from LD simulations which are carried out until the system reaches either the interface λ_{i+1} or the basin \mathbf{A} , i.e., without restricting the simulation time. In the MCH formalism this corresponds to the probability that the system, being initially in the i th state, will be found in the $(i+1)$ th state after an arbitrarily large number of steps (equilibrium configuration). Thus, in order to compute $w_{i \rightarrow i+1}$ from the one-step matrix $\hat{\mathbf{P}}^{(i+1)}$, we have to find the matrix $\hat{\mathbf{E}}^{(i+1)} = \lim_{k \rightarrow \infty} (\hat{\mathbf{P}}^{(i+1)})^k$. The probability of interest is then given by the corresponding matrix element of $\hat{\mathbf{E}}^{(i+1)}$, namely $w_{i \rightarrow i+1} = E_{i,i+1}^{(i+1)}$.

Importantly, the limit $\lim_{k \rightarrow \infty} (\hat{\mathbf{P}}^{(i+1)})^k$ can be computed very fast: after the diagonalization of $\hat{\mathbf{P}}^{(i+1)} = \hat{\mathbf{Q}} \hat{\mathbf{D}} \hat{\mathbf{Q}}^{-1}$ this limit becomes $\lim_{k \rightarrow \infty} (\hat{\mathbf{P}}^{(i+1)})^k = \lim_{k \rightarrow \infty} \hat{\mathbf{Q}} \hat{\mathbf{D}}^k \hat{\mathbf{Q}}^{-1}$, so that we have to evaluate only the limits $\lim_{k \rightarrow \infty} d_j^k$ for eigenvalues of the matrix $\hat{\mathbf{P}}^{(i+1)}$. According to the properties of stochastic matrices, all their eigenvalues obey the inequality $d_i \leq 1$, so that corresponding limits are either 0 or 1.

B. Assignment of one-step probabilities $\{p\}$ and $\{q\}$

To assign the one-step probabilities $p_{i \rightarrow i+1}$ and $q_{i+1 \rightarrow i}$ for the Markov chain, we have first to establish the correspondence between the energy landscape and the MCH states. In our previous paper [35] we have proposed to place

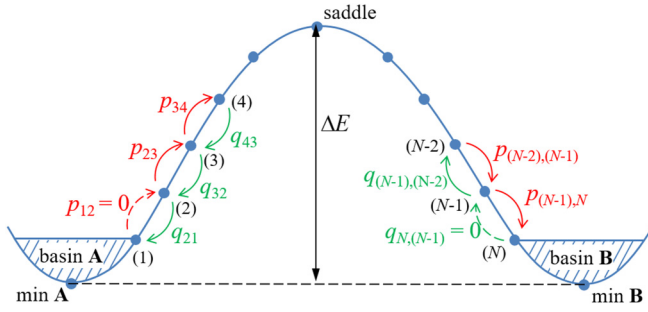


FIG. 3. Correspondence between the Markov chain states and the two-minima energy landscape.

the interfaces for FFS simulation of the transition $A \rightarrow B$ not according to the values of magnetic moment projections (as it is done usually [31,32]), but equidistantly in the energy space of the studied system. This positioning has greatly simplified the FFS algorithm, because the probabilities $w_{i \rightarrow i+1}$ depend mainly on the energy differences between the interfaces: $w_{i \rightarrow i+1} \sim \exp[-(E_{i+1} - E_i)/kT]$. Hence, for energy-equidistant interfaces these probabilities should be approximately the same for all “uphill” interface pairs $i \rightarrow i+1$, which should minimize the statistical error of FFS [29,30].

In our EDT algorithm presented here, we use the same principle to position the interfaces and correspondingly Markov chain states, as shown in Fig. 3.

This interface placement allows us to assign the MCH probabilities $p_{i \rightarrow i+1}$ and $q_{i+1 \rightarrow i}$ using the thermodynamical principle of the detailed balance (see, e.g., [39]). According to this principle, one-step MCH probabilities $p_{i \rightarrow j}$ and $q_{j \rightarrow i}$ are related to the equilibrium probabilities to find the system in the corresponding states π_i and π_j as $\pi_i p_{i \rightarrow j} = \pi_j q_{j \rightarrow i}$. Furthermore, in a thermodynamic equilibrium these latter probabilities are given by $\pi_i \simeq n_i \exp(-E_i/k_B T)$, where $n_i = n(E_i)$ is the number of states per unit energy, i.e., the density of states (DoS) at the energy E_i . Hence, one-step MC probabilities $p_{i \rightarrow i+1}$ and $q_{i+1 \rightarrow i}$ should obey the relation

$$\frac{p_{i \rightarrow i+1}}{q_{i+1 \rightarrow i}} = \frac{\pi_{i+1}}{\pi_i} = \frac{n_{i+1} e^{-E_{i+1}/k_B T}}{n_i e^{-E_i/k_B T}} = \frac{n_{i+1}}{n_i} \exp\left(-\frac{\delta E_{i,i+1}}{k_B T}\right), \quad (8)$$

where $\delta E_{i,i+1} = E_{i+1} - E_i$.

To satisfy this relation, we set

$$p_{i \rightarrow i+1} = \left(\frac{n_{i+1}}{n_i}\right)^{1/2} \exp\left(-\frac{1}{2} \frac{\delta E_{i,i+1}}{k_B T}\right), \quad (9)$$

$$q_{i+1 \rightarrow i} = \left(\frac{n_i}{n_{i+1}}\right)^{1/2} \exp\left(+\frac{1}{2} \frac{\delta E_{i,i+1}}{k_B T}\right). \quad (10)$$

To evaluate the ratio of DoS n_{i+1}/n_i for two subsequent states we note that for a small energy increments $\delta E_{i,i+1} \equiv \delta E$ we can expand $n_{i+1} = n(E_{i+1})$ into the Taylor series near $E = E_i$, obtaining

$$n_{i+1} = n_i + \left. \frac{\partial n}{\partial E} \right|_{E=E_i} \delta E = n_i \left(1 + \frac{\delta E}{n_i} \left. \frac{\partial n}{\partial E} \right|_{E=E_i}\right) \quad (11)$$

so that the required ratio becomes

$$\left(\frac{n_{i+1}}{n_i}\right)^{\pm 1/2} = 1 \pm \frac{\delta E}{2n_i} \left. \frac{\partial n}{\partial E} \right|_{E=E_i}. \quad (12)$$

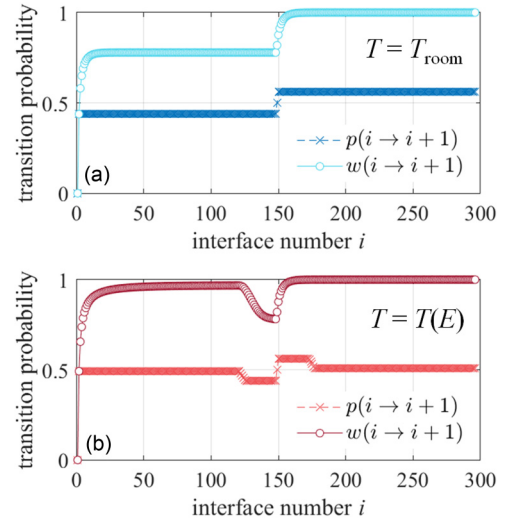


FIG. 4. One-step probabilities $p_{i \rightarrow i+1}$ (lines with crosses) and total probabilities $w_{i \rightarrow i+1}$ (lines with circles) as functions of the interface number for $T = T_{\text{room}}$ (a) and $T = T(E)$ (b).

Thus, for energies where the DoS $n(E)$ is nonsingular (which is normally the case if E does not correspond to an extremum of a saddle point) we can set $n_{i+1}/n_i \approx 1$ for small $\delta E \rightarrow 0$. Finally, we have to normalize p 's and q 's so that $p_{i \rightarrow i+1} + q_{i \rightarrow i-1} = 1$ as mentioned above.

IV. VALIDATION OF THE EDT ALGORITHM

Dependencies of probabilities p_i on the interface number i for the whole Markov chain are shown in Fig. 4 for $T = T_{\text{room}} = \text{const.}$ and $T = T(E)$ (1) as lines marked with crosses; in this example here the barrier is $\Delta E = 38k_B T$ and the interface distance $\delta E = 0.25k_B T$ ($q_i = 1 - p_i$ and thus are not shown).

According to the definition (9), for $T = \text{const.}$ one-step probabilities p_i should exhibit a jump for the interface corresponding to the saddle point [i.e., the middle interface in Fig. 4(a)], because at this point the energy difference $E_{i+1} - E_i$ changes its sign. According to Eq. (1) and Fig. 1, the values of p_i 's should rapidly change also around the interfaces corresponding to the energy $E_{\text{cool}} = \Delta E - b_{\text{cool}} k_B T$ [line with crosses in Fig. 4(b)], where the temperature drops from T_{lg} to T_{room} .

Total transition probabilities $w_{i \rightarrow i+1}$ obtained from these one-step quantities as explained above [i.e., as $w_{i \rightarrow i+1} = E_{i,i+1}^{(i+1)}$, where $\hat{\mathbf{E}}^{(i+1)} = \lim_{k \rightarrow \infty} (\hat{\mathbf{P}}^{(i+1)})^k$ with the matrix $\hat{\mathbf{P}}$ given by (7)], are shown in the same Fig. 4 as lines marked by circles. It can be seen that after the jump of p_i the total probability $w_{i \rightarrow i+1}$ changes *smoothly*, tending to its new limit for the new constant temperature: $w_{i \rightarrow i+1} \rightarrow \exp(-\delta E/k_B T)$ for $\delta E > 0$ [35]. This behavior is in accordance with the physical sense of the quantity $w_{i \rightarrow i+1}$ defined as the result of an unlimited number of steps for the MCH with the matrix (7). For example, it is clear that the total probability $w_{i \rightarrow i+1}$ to reach the next interface, i.e., not to return back to the basin A, should gradually increase when the distance to this basin increases.

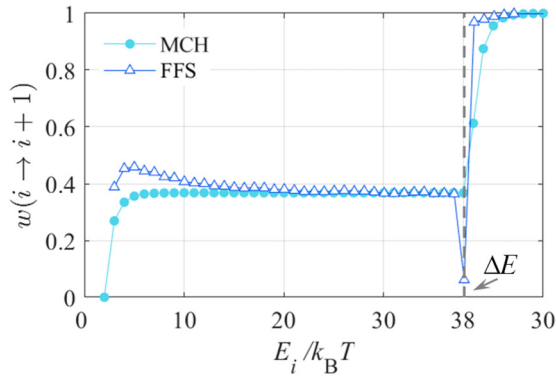


FIG. 5. Total transition probabilities $w_{i \rightarrow i+1}$ for FFS (open triangles) and MCH (closed circles) methods for the constant temperature $T = 300$ K (system with $\Delta E/k_B T = 38$ and $\delta E/k_B T = 1$).

The behavior of MCH probabilities $w_{i \rightarrow i+1}$ can be better understood by comparing them to analogous quantities calculated via the FFS with the same energy-equidistant interfaces (see [35] for the details of the latter method). Results of this comparison for the system with $\Delta E/k_B T = 38$ and interface distance $\delta E/k_B T = 1$ are shown for $T = \text{const.}$ in Fig. 5 and for the EDT (1) in Fig. 6.

First we note that in both cases the difference between probabilities obtained by MCH and FFS for interface energies well below the saddle point is due to the rather large value of the interface distance ($\delta E = 1k_B T$) used here. For such δE neglecting the change of $n(E)$ in the expansion (12) has a noticeable effect. We have checked that this difference decreases with $\delta E \rightarrow 0$, as it should be. Furthermore, we note that for this particular model it is possible to evaluate DoS and to take the corresponding correction into account by evaluating one-step and total transition probabilities. With this correction, MCH and FFS probabilities $w_{i \rightarrow i+1}$ coincide for energies below the saddle. However, as we aim to develop a universal method which should be also suitable for more complicated models where the evaluation of DoS requires a substantial effort, we did not introduce this correction here.

The energy dependence of total probabilities $w_{i \rightarrow i+1}$ in the EDT method shown in Figs. 4 and 6 provides an additional condition for the choice of the EDT parameters $a_{\text{lr}}g$ and b_{cool} . Namely, the probability $w_{i \rightarrow i+1}(E)$ should be allowed

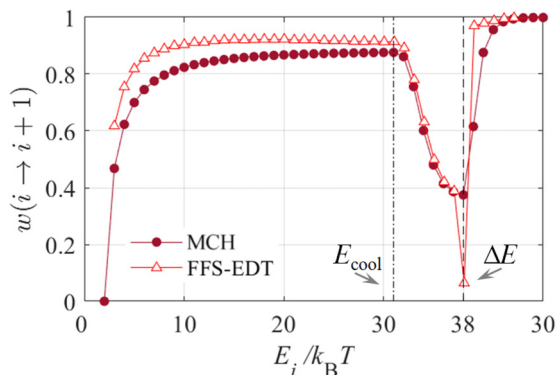


FIG. 6. The same as in Fig. 5 for the energy-dependent temperature $T(E)$ given by (1).

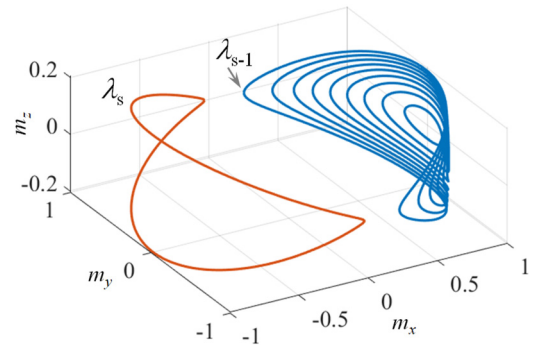


FIG. 7. To the explanation of the dip on the dependencies $w_{i \rightarrow i+1}(E_i)$ in Figs. 5 and 6: the interface λ_{s-1} immediately before the saddle point and the next (saddle) interface λ_s are separated by a large distance in the coordinate space.

“relax” to its “normal” value for $T = T_{\text{room}}$ starting from a much higher value for $T = T_{\text{lr}}g$. This requirement poses the lower limit on the values of b_{cool} (to make the difference $\Delta E - E_{\text{cool}} = b_{\text{cool}}k_B T$ large enough) and $a_{\text{lr}}g$ (so that the value of $T_{\text{lr}}g$ is not too high). We emphasize that checking the fulfillment of this condition does not require any LD simulations, but merely the evaluation of MCH probabilities as explained above.

Next, we consider the most important feature of $w_{i \rightarrow i+1}$ seen in Figs. 5 and 6: the large discrepancy between MCH and FFS probabilities at and slightly above the saddle point energy ΔE . This discrepancy reflects the qualitative difference between the FFS and MCH methods. Namely, in FFS we evaluate $w_{i \rightarrow i+1}$ by LD simulations taking into account complicated physical processes near the saddle point (back-hopping in the first place) and the peculiarities of FFS interfaces for the specific system under study. In particular, for our macrospin the probability to reach the saddle-point interface λ_s is especially small (see large dips at $E_i = \Delta E$ on w_i dependencies for FFS in Figs. 5 and 6), because the conditions to reach this interface also include the requirement that m_x -projection changes its sign (see [35] for details). For this reason the distance between the interface λ_s and the previous one in the coordinate space is much larger than for preceding interface pairs (see Fig. 7), leading to the correspondingly small probability $w(\lambda_{s-1} \rightarrow \lambda_s)$. For the same reason, $w_{i \rightarrow i+1}$ strongly increases immediately after this interface, because the probability to return to previous interfaces (before the saddle point) is very low.

In contrast, in MCH we merely compute the limit $\hat{\mathbf{E}}^{(i+1)} = \lim_{k \rightarrow \infty} (\hat{\mathbf{P}}^{(i+1)})^k$ where one-step probabilities p_i and q_i constituting the matrix $\hat{\mathbf{P}}$ exhibit only a relatively small jump near the saddle point, so that $w_{i \rightarrow i+1}$ do not show any dip at this interface and change after λ_s much slower than for FFS.

However—and this is the key point of our method—the ratio of probabilities $w_{i \rightarrow i+1}^{\text{EDT}}/w_{i \rightarrow i+1}^{\text{CT}}$ should be the same (in the limit $\delta E \rightarrow 0$) in both FFS and MCH methods for all interface energies, including the region near the saddle point.

This statement follows directly from the construction of the energy-dependent temperature (1), where $T(E) \rightarrow T_{\text{room}}$ for $E \simeq \Delta E$. Due to this behavior of $T(E)$ one-step MCH probabilities (9) and (10) near the saddle point should be the

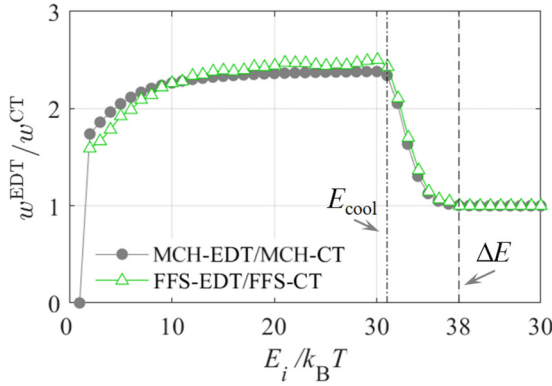


FIG. 8. Ratio of probabilities $w_{i \rightarrow i+1}^{\text{EDT}}/w_{i \rightarrow i+1}^{\text{CT}}$ for FFS (open triangles) and MCH (full circles) methods as a function of the interface energy. A very good agreement of these ratios for both methods is clearly demonstrated.

same for $T = \text{const.}$ and EDT. Hence, as long as b_{cool} is large enough to allow $w_{i \rightarrow i+1}$ (computed from the matrix $\hat{\mathbf{E}}^{(i+1)}$) to reach its steady-state value for $T = T_{\text{room}}$ in the saddle point region, in this region we should obtain $w_{i \rightarrow i+1}^{\text{EDT}} = w_{i \rightarrow i+1}^{\text{CT}}$. In the FFS method, probabilities w are obtained from LD simulations, which “feel” at each time integration step only the local temperature, so these probabilities should also be equal in the saddle-point region for $T = \text{const.}$ and $T(E)$ cases.

Corresponding ratios $w_{i \rightarrow i+1}^{\text{EDT}}/w_{i \rightarrow i+1}^{\text{CT}}$ are plotted in Fig. 8 for the same system as in Figs. 5 and 6. It can be clearly seen that these ratios for FFS and MCH methods agree very well for all interface energies—both well below the saddle point (where these ratios are governed only by the local temperatures) and in the saddle point region, where the dynamics of a real system plays a decisive role in the FFS method. This means that the ratio of the probability products (6) required for the evaluation of the switching time in our EDT concept *can be computed using the matrix chain method*. As stated above, this computation is very fast, involving only the diagonalization of matrices $\hat{\mathbf{P}}^{(i+1)}$. Moreover, the ratio r computed this way depends only on the function $T(E)$ and thus can be evaluated for any system with the given barrier ΔE once and for all.

Hence our algorithm for the switching time evaluation requires only numerical simulations of transitions over the barrier for the studied system with the *energy-dependent* temperature, whereby we have to collect a sufficiently accurate statistics of transitions over the effective barrier with the height $\Delta E_{\text{eff}} \simeq \Delta E - E_{\text{cool}} = b_{\text{room}} k_B T$. Corresponding simulation time t_{sim} is not only easily accessible for the direct LD modeling, but should be approximately *independent* on the height of the actual barrier ΔE —in strong contrast both to standard LD simulations [where $t_{\text{sim}} \sim \exp(\Delta E/k_B T)$] and FFS methods ($t_{\text{sim}} \sim \Delta E$).

Moreover, our method does suffer from the instability problem arising in FFS, energy bounce, and other multistage algorithms due to the presence of the product of numerically computed transition probabilities, as explained in detail in the Introduction. Computation of the probability product ratio r (6) in our method is error free, so that this instability is completely absent.

Summarizing, our algorithm consists of the following stages:

(s1) Compute the energy barrier ΔE between the basins **A** and **B** and divide the path between them into N states with the energy differences δE between them.

(s2) Set the energy-dependent temperature (1).

(s3) Using this $T(E)$ dependence, assign the one-step hopping probabilities $\{p_i\}$ and $\{q_i\}$ between the states according to Eqs. (9) and (10).

(s4) For each state i , build the transition matrix $\hat{\mathbf{P}}^{i+1}$ given by Eq. (7) for the corresponding Markov chain.

(s5) Compute the total EDT transition probabilities as matrix elements $w_{i \rightarrow i+1}^{\text{EDT}} = E_{i,i+1}^{(i+1)}$, where $\hat{\mathbf{E}}^{(i+1)} = \lim_{k \rightarrow \infty} (\hat{\mathbf{P}}^{(i+1)})^k$ using the diagonalization of matrices $\hat{\mathbf{P}}^{(i+1)}$.

(s6) Repeat steps (s3)–(s5) for the constant temperature $T = T_{\text{room}}$ to obtain the probabilities $w_{i \rightarrow i+1}^{\text{CT}}$.

(s7) Perform LD simulations for the EDT case and compute the EDT switching time $\tau_{\text{sw}}^{\text{EDT}}$ in a standard way.

(s8) Perform LD simulations for $T = T_{\text{room}}$ and $T = T_{\text{lg}}$ to compute the corresponding fluxes Φ_0^{CT} and Φ_0^{EDT} out of the basin **A**.

(s9) Compute the real switching time (for the constant temperature) $\tau_{\text{sw}}^{\text{CT}}$ using Eq. (5).

We emphasize once more that *the only really time-consuming step* in this algorithm is step (s7), where an accurate statistics of the switching events for the system with EDT should be collected.

V. PHYSICAL RESULTS AND COMPARISON OF EDT WITH FFS

To demonstrate the high accuracy of our algorithm and to quantitatively compare the simulation time for determination of the switching rate in the EDT paradigm with the corresponding time required by FFS, we have simulated with both methods the same series of macrospins with the biaxial anisotropy as analyzed in [35]: with magnetic parameters as for Permalloy (magnetization $M = 800$ G, damping $\lambda = 0.01$) and demagnetizing factors of flat nanoellipses with the thickness $h = 3$ nm, short axis $b = 40$ nm, and long axes a varying from 50 to 100 nm. Corresponding energy barriers are in the range $9 \leq \Delta E/k_B T \leq 60$, so that switching times for these macrospins cover approximately 20 orders of magnitude.

As shown in Fig. 9, our method demonstrates an excellent agreement with FFS simulations in the whole range of energy barriers. We note that when only $\tau_{\text{sw}}(\Delta E)$ dependencies obtained with various methods are plotted [Fig. 9(a)], some discrepancies can be masked by the strong exponential term necessarily present in all methods. For this reason, in Fig. 9(b) we have displayed the ratios of the FFS and EDT switching times to the analytical result obtained for the same biaxial macrospins in our previous paper [35] (the latter result was derived basing on the advanced formalism outlined in [20]). This comparison, where the term $\exp(\Delta E/k_B T)$ is canceled out, clearly demonstrates a very good agreement between our EDT formalism and the standard FFS method.

Finally, to compare the performance of our algorithm and the FFS method, we have determined simulation times

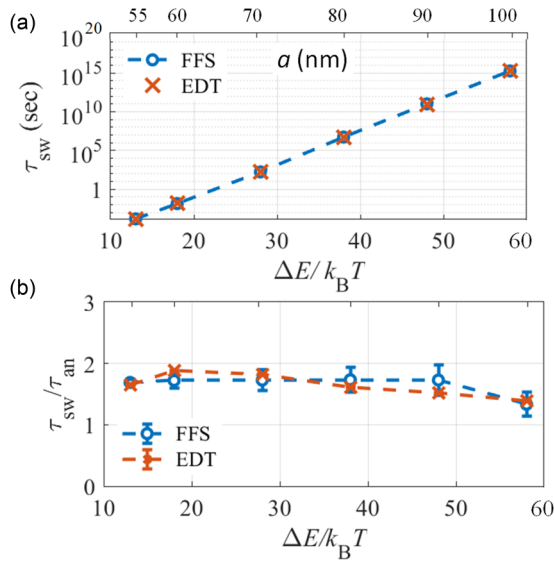


FIG. 9. Switching times computed by the standard ($T = \text{const.}$) FFS method (red open circles) compared to the same times obtained via EDT. An excellent agreement between both methods is clearly demonstrated.

required to compute τ_{sw} with the relative accuracy $\epsilon = 5\%$ with both methods. Results of this comparison plotted in Fig. 10 confirm our conclusions drawn above. Namely, the FFS simulation time growth is approximately linear with the barrier height ΔE , because the time required to compute each probability w_i is approximately the same for each interface, and the required number of interfaces grows linearly with ΔE . For our EDT algorithm, simulation time even decreases somewhat when the barrier increases, because for higher barriers the temperature T_{lg} should be higher to ensure the same values of the probability $p(E_{\text{cool}})$ (see Sec. II A), so that the

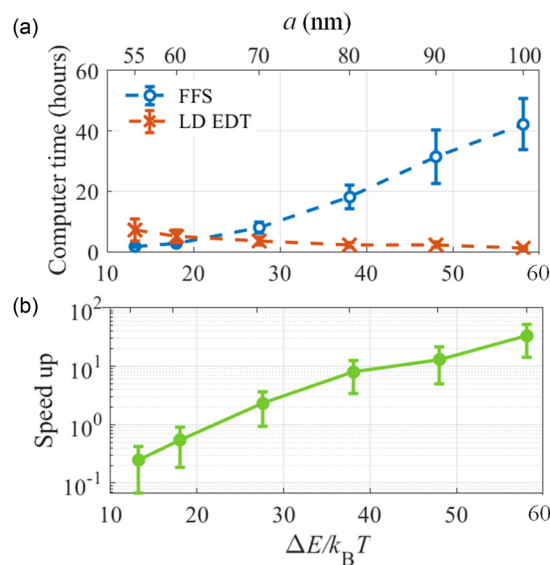


FIG. 10. Computation times (a) and speedup of the EDT method as compared to FFS. In both methods, LD with the constant time step $\Delta t = 0.001$ was used to achieve the relative accuracy of 5% for τ_{sw} .

number of transitions over the barrier per unit time in EDT-LD simulations also increases. Thus we need smaller simulation time to obtain the statistics of the same quality.

The speedup of the EDT algorithm compared to FFS is shown in Fig. 10(b): the break point is achieved already for a very moderate barrier $\Delta E/k_B T \approx 20$, and for the highest studied value $\Delta E/k_B T \approx 60$ our method is more than 40× faster than FFS.

Finally, we point out that our method allows a straightforward generalization to systems with an arbitrary number of degrees of freedom, in particular, to strongly interacting many-particle systems and discrete models of continuous bodies (like full-scale micromagnetics). In the sequence of steps listed at the end of Sec. IV only the evaluation of the energy barrier ΔE (s1) and LD simulations (s7) and (s8) are system specific, all other steps do not require any additional adjustments. The energy barrier between two metastable states of interest is always needed. For systems where it cannot be found analytically—as it would be the case in the majority of applications—this task can be accomplished using one of numerical methods listed in the Introduction (e.g., the “nudged elastic band” method which is widely used for this purpose for a large variety of systems). Based on the value of this energy barrier, we can then define a suitable energy-dependent temperature in the form given by the Eq. (1). Lastly, LD simulations should be readily available for any system, as they require only the knowledge of forces acting on the system particles (or torques acting on magnetic moments).

VI. CONCLUSION

In this paper we have introduced the concept of the energy-dependent temperature (EDT), which allows us to simulate transitions over *arbitrarily high* energy barriers by *single-stage* Langevin dynamics simulations. Our method has been verified on the example of a biaxial magnetic macrospin—the archetypal magnetic system with two energy minima and two equivalent saddle points—where our results agree very well with switching times obtained via the forward flux sampling (FFS). We have shown that the computation time for the EDT-based LD simulations *does not increase* with the energy barrier height, in contrast to FFS and other “climbing” methods, thus providing a unique possibility to simulate transitions over any barrier with a very moderate numerical effort. The speedup of our LD-EDT method in comparison with the (strongly optimized) FFS algorithm achieves 40× for the energy barrier of $\approx 60k_B T$. Furthermore, the presented EDT-LD algorithm does not require the evaluation of the product of a large number of conditional probabilities for transitions between subsequent interfaces as in FFS and related methods (like “energy bounce,” etc. [35]) and thus does not suffer from the stability problem arising due to this procedure in the presence of any systematic error occurring by the computation of these probabilities.

ACKNOWLEDGMENT

Financial support of the Deutsche Forschungsgemeinschaft (German Research Foundation) DFG-project BE 2464/18-1 is greatly acknowledged.

- [1] P. Haenggi, P. Talkner, and M. Borkovec, *Rev. Mod. Phys.* **62**, 251 (1990).
- [2] B. Peters, *Reaction Rate Theory and Rare Events* (Elsevier B.V., Amsterdam, 2017).
- [3] R. Cabriolu, K. Refsnes, P. Bolhuis, and T. van Erp, *J. Chem. Phys.* **147**, 152722 (2017).
- [4] J. Wales, *Annu. Rev. Phys. Chem.* **69**, 401 (2018).
- [5] S. Hussain and A. Haji-Akbari, *J. Chem. Phys.* **152**, 060901 (2020).
- [6] G. Bussi, A. Laio, and P. Tiwary, Metadynamics: A unified framework for accelerating rare events and sampling thermodynamics and kinetics, in *Handbook of Materials Modeling*, edited by W. Andreoni and S. Yip (Springer, Switzerland AG, 2020), Chap. 27, p. 565.
- [7] H. Jonsson, G. Mills, and K. Jacobsen, Nudged elastic band method for finding minimum energy paths of transitions, in *Classical and Quantum Dynamics in Condensed Phase Simulations* (World Scientific, Singapore, 1998), Chap. 16, pp. 385–404.
- [8] P.-A. Geslin, R. Gatti, B. Devincere, and D. Rodney, *J. Mech. Phys. Solids* **108**, 49 (2017).
- [9] H. Herbol, J. Stevenson, and P. Clancy, *J. Chem. Theory Comput.* **13**, 3250 (2017).
- [10] A. V. Ivanov, D. Dagbartsson, J. Tranchida, V. M. Uzdin, and H. Jónsson, *J. Phys.: Condens. Matter* **32**, 345901 (2020).
- [11] L. Zhao, K. Watanabe, N. Nakatani, A. Nakayama, X. Xu, and J. Hasegawa, *J. Chem. Phys.* **153**, 134114 (2020).
- [12] V. Ásgeirsson, B. Birgisson, R. Björnsson, U. Becker, F. Neese, C. Riplinger, and H. Jónsson, *J. Chem. Theory Comput.* **17**, 4929 (2021).
- [13] W. E, W. Ren, and E. Vanden-Eijnden, *Phys. Rev. B* **66**, 052301 (2002).
- [14] D. Berkov, Magnetization dynamics including thermal fluctuations, in *Handbook of Magnetism and Advanced Magnetic Materials*, edited by H. Kronmüller and S. Parkin (John Wiley & Sons, 2007), Vol. 2, Chap. 4, pp. 795–823.
- [15] L. Onsager and S. Machlup, *Phys. Rev.* **91**, 1505 (1953).
- [16] D. Berkov, *J. Magn. Magn. Mater.* **186**, 199 (1998).
- [17] H.-B. Braun, *J. Appl. Phys.* **76**, 6310 (1994).
- [18] G. Fiedler, J. Fidler, J. Lee, T. Schrefl, R. L. Stamps, H. Braun, and D. Suess, *J. Appl. Phys.* **111**, 093917 (2012).
- [19] H. Kramers, *Physica* **7**, 284 (1940).
- [20] W. Coffey and Y. Kalmykov, *J. Appl. Phys.* **112**, 121301 (2012).
- [21] V. Mel'nikov and S. Meshkov, *J. Chem. Phys.* **85**, 1018 (1986).
- [22] W. F. Brown Jr, *IEEE Trans. Magn.* **15**, 1196 (1979).
- [23] I. Klik and L. Gunther, *J. Stat. Phys.* **60**, 473 (1990).
- [24] W. T. Coffey, D. A. Garanin, and D. J. McCarthy, Crossover formulas in the kramers theory of thermally activated escape rates—application to spin systems, *Advances in Chemical Physics*, edited by I. Prigogine and S. A. Rice, Vol. 117 (Wiley, 2001), p. 483.
- [25] P. M. Déjardin, D. S. F. Crothers, W. T. Coffey, and D. J. McCarthy, *Phys. Rev. E* **63**, 021102 (2001).
- [26] A. Hubert, *Magnetic Domains: The Analysis of Magnetic Microstructures* (Springer, Berlin, 1998).
- [27] R. J. Allen, P. B. Warren, and P. R. ten Wolde, *Phys. Rev. Lett.* **94**, 018104 (2005).
- [28] R. J. Allen, D. Frenkel, and P. R. ten Wolde, *J. Chem. Phys.* **124**, 194111 (2006).
- [29] E. E. Borrero and F. A. Escobedo, *J. Chem. Phys.* **129**, 024115 (2008).
- [30] R. Allen, C. Valeriani, and P. R. ten Wolde, *J. Phys.: Condens. Matter* **21**, 463102 (2009).
- [31] C. Vogler, F. Bruckner, B. Bergmair, T. Huber, D. Suess, and C. Dellago, *Phys. Rev. B* **88**, 134409 (2013).
- [32] C. Vogler, F. Bruckner, D. Suess, and C. Dellago, *J. Appl. Phys.* **117**, 163907 (2015).
- [33] L. Desplat and J.-V. Kim, *Phys. Rev. Appl.* **14**, 064064 (2020).
- [34] L. Desplat, C. Vogler, J.-V. Kim, R. L. Stamps, and D. Suess, *Phys. Rev. B* **101**, 060403(R) (2020).
- [35] E. K. Semenova, D. V. Berkov, and N. L. Gorn, *Phys. Rev. B* **102**, 144419 (2020).
- [36] S. Wang and P. Visscher, *J. Appl. Phys.* **99**, 08G106 (2006).
- [37] D. Berkov, E. K. Semenova, and N. L. Gorn, *Phys. Rev. Lett.* **127**, 247201 (2021).
- [38] R. Howard, *Dynamic Probabilistic Systems: Markov Models* (J. Wiley & Sons, New York, 2012).
- [39] N. van Kampen, *Stochastic Processes in Physics and Chemistry* (Elsevier Science, Amsterdam, 1992).